

# Effects of Curvature on Spacecraft Propellant Management Surface Tension Screen Capillary Capability

Phil MacEachron<sup>1</sup>, Emma Alexander<sup>2</sup>, Nafeesa Khan<sup>3</sup>, and Manjari Randeria<sup>4</sup>  
*Yale University*

Jonathan P. Braun<sup>5</sup> and Christine Stewart<sup>6</sup>  
*Lockheed Martin Space Systems Company*

**In the development and operations of spacecraft, the application of a propellant management device, or PMD, is one solution to mitigate propellant slosh and deliver gas free propellant to the system’s engines. PMDs range in complexity and are unique to every propulsion system, but a large subset of PMDs use surface tensions screens to directly control the location of gas, and indirectly the location of the liquid, in the tank. The limiting capability of any surface tension screen is defined by its “bubble point,” or the differential pressure at which the surface tension of the liquid propellant on the screen breaks and gas bubbles through. The propellant management community has identified that curving a surface tension screen alters its bubble point, but the effect of curvature isn’t easily quantified and the problem is typically overcome by overdesigning the system to ensure its proper function. This overdesign can cost the system in terms of weight, money, performance, and general uncertainty. The purpose of this investigation was to quantify the effects of curvature on the bubble point of several typical types of surface tension screen. Through NASA’s SEED program, the bubble point was tested in a microgravity environment for three screen types at four different curvatures. The microgravity environment enabled uniform pressure across the screens, so that the bubble point was tested across the entire screen’s surface. Even though the data is noisy, the results show a trend in sensitivity of the bubble point, with a notable degradation in performance as the screen curvature increases. Method, testing procedure, and lessons learned are discussed. The resulting curves from the data of this project can potentially help in PMD design efforts and give insight into this important on-orbit effect.**

## Nomenclature

|              |   |  |
|--------------|---|--|
| $P_{Liquid}$ | = | Pressure on liquid side of surface tension screen            |
| $P_{Gas}$    | = | Pressure on gas side of surface tension screen               |
| $P_h$        | = | Hydrostatic pressure of liquid column                        |
| $P_{amb}$    | = | Ambient pressure (atmospheric)                               |
| $F_g$        | = | Force of gravity   |
| $\Delta P$   | = | Pressure differential across a wetted surface tension screen |

---

<sup>1</sup> Undergraduate Research Associate, Department of Physics, Yale University, AIAA Student Member

<sup>2</sup> Graduate Research Associate, Department of Computer Science, School of Engineering and Applied Science, Harvard University

<sup>3</sup> Undergraduate Research Associate, Department of Biomedical Engineering, Yale University

<sup>4</sup> Undergraduate Research Associate, Department of Physics, Yale University

<sup>5</sup> Liquid Propulsion Subsystems Associate Manager, Lockheed Martin Space Systems Company, Sunnyvale, CA, AIAA Senior Member.

<sup>6</sup> Senior Systems Engineer, Lockheed Martin Space Systems Company, Denver, CO, AIAA Professional Member.

## I. Introduction

**I**N the field of spacecraft liquid propulsion subsystems, propellant management devices (PMDs) are a mass efficient and reliable method of liquid propellant control. While the vast majority of fluids problems in common experience are dominated by gravity, PMDs are designed to operate in microgravity environments where surface tension effects govern the activity of the liquid. Propellant management devices cover a broad range of designs with common goals in one or more of the following categories: Provide the propulsion subsystem with pressurant-free propellant flow, provide propellant slosh control for the spacecraft, limit the effects of propellant motion on vehicle attitude and dynamics, and provide propellant motion/location knowledge to the ground team for their assistance to estimation of propellant mass status. PMDs must have high reliability, low weight, and excellent long term compatibility with spacecraft propellants.

Depending on mission requirements, PMD designs can vary greatly. Some categories of PMD designs include vanes<sup>1</sup>, diaphragms<sup>1</sup>, traps/troughs<sup>3</sup>, sponges<sup>2</sup>, and gallery arms<sup>4</sup>. The Orion Crew Module propellant tanks contain a diaphragm type PMD while the Orion Service Module contains a combination trap/gallery arm PMD due primarily to the high maneuverability requirements of the mission. In contrast, the MESSENGER program uses a vane PMD device, as do most commercial communications satellites, in a relatively low perturbation environment.

Two varieties of PMDs, gallery arms and traps/troughs, often contain either titanium or stainless steel surface tension screens. Surface tension screens act as a limited boundary through which liquid can pass, and gaseous compounds cannot, when completely wetted. Based on the principles of capillary physics, surface tension screens are limited in capability by their bubble point – the maximum pressure differential across the screen prior to free gas transfer. The bubble point, or capillary capability, of any given screen generally increases with the number of wires (chutes and weave) per square inch and is inversely proportional to pore size (Figure 1). The higher the bubble point of a screen, the more effective it is at controlling propellant and gas locations. However, the consequences for implementing a surface tension screen with a high bubble point includes increased pressure losses during flow through the screen<sup>4</sup>; which presents as higher propellant residuals, thereby reducing the performance of the propulsion subsystem. Additionally, the screens with higher bubble point capability typically use smaller wires which are more susceptible to fretting or fatigue failure.

To mitigate these performance reductions, the requirements for surface tension screens are analyzed precisely to avoid over designing the system. However, known - but yet unquantified - effects which negatively impact the bubble point of the surface tension screen drive the industry to apply a standard design margin. A clearer, more quantitative understanding of screen bubble point reduction will allow engineers to more effectively analyze these systems and lower margins where needed.

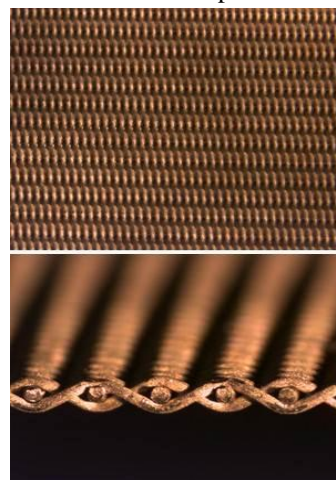


**Figure 1. Image of screen weave in a plain dutch surface tension screen (22x110; Titanium).**

## II. Experiment Definition

### A. Physics of Experiment

Surface tension screens, as implied by the name, rely upon the physical principles of surface tension to accomplish the goal of keeping liquid (propellant) and gas (pressurant) separated in a spacecraft propulsion system. In a propellant management device, the low contact angle of the propellant creates a situation where the liquid phase “adheres” to solid surfaces with the desire to minimize the static energy of the liquid by evenly distributing the surface pressure of the liquid phase. Surface tension screens are designed to make use of this wetting property as the contacting propellant wets the entire surface of the screen, as long as sufficient liquid volume exists and as long as

transverse external forces don't overcome the adhering energy of the low contact angle surface tension.

Once the propellant has completely wet the surface of the screen, any gas must apply adequate force on the wetted capillary to push through the surface energy of the liquid. The force applied to the liquid surface is measured as pressure differential over the capillary area with the pass-through pressure being a function of both the capillary size and the surface energy of the liquid – i.e. a liquid with a higher surface tension will also produce a higher surface energy for the gas to overcome. The pressure differential required for gas to push past an individual surface tension screen capillary defines the maximum capability of that screen to keep the gas and liquid phase separate and is termed the bubble point (equation 1; Figure 2). It's important to note, in Figure 2, when neglecting external forces, the substance above the screen can be liquid or gas as long as the screen is fully wetted.

$$\Delta P = P_1 - P_2 \quad (1)$$

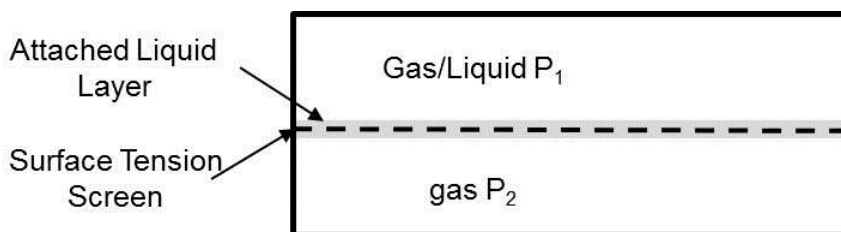


**Figure 2. Description of surface tension screen boundary with developed pressure differential.**

The capillary geometry generated by most surface tension screen weaves is not an idealized circular pore, but is typically more triangular and complex. Since the bubble point of the screen is highly dependent on the pore geometry, as well as the fluid topology, computer tools such as *Surface Evolver*, and *Flow3D*, are inadequate in calculating a numerical value for the resulting screen bubble point. Computer modeling is also difficult because there are thousands of pores in a single screen segment – with the largest pore contributing to the minimum bubble point. Because of these challenges in computer modeling, testing for surface tension screens is a more accurate and cost effective method for determining capillary capability.

## B. Experiment Goals

The goal of this experiment was to quantify the effect of screen curvature on surface tension screens by testing in a microgravity environment, where the effects of inconsistent hydrostatic pressure can be eliminated. In effect, the aim was to develop a quantifiable relationship of screen radius of curvature to the bubble point, or capillary capability, of the screen. Initially, the goal was to evaluate the impact of both concave and convex curvature. However, due to the test duration constraints, the authors opted for a greater sample size in the convex orientation – the orientation most common in practice.

Since bubble-point testing in a microgravity environment has been unsuccessfully attempted multiple times in the past, an ancillary goal was to capture the lessons learned incrementally through the process. These lessons are discussed in Section V and include: test fluid/cell material compatibility, test cell sealing techniques, high resolution pressure measurement, non-welding screen sealing techniques, etc.

The investigation incorporated tests for two different weaves of titanium screen, the most common material used in industry, and one fine weave composed of stainless steel. Each of the screen types had four representative samples tested at multiple radii of curvature. Nominal testing was completed for each of the screen segments in the flat, uncurved, orientation as a baseline for comparison against the curved tests. The radii of curvature chosen for this study were 4 inches, 3 inches, 2 inches, and 1 inch.

### **C. Hypothesis**

Surface tension screens operate on the principle that smaller cross sectional pore sizes have larger bubble points; i.e. the screen's performance is reduced as pore sizes increase. The nominal, best case, performance of a surface tension screen is a perfectly distributed weave in which the maximum pore size is also the minimum pore size. Since pressure is evenly applied across the entire screen in a microgravity environment, the screen is only as capable as the largest pore size. The large quantity of pores, often numbering in the thousands, in a single surface tension screen leads to the statistical likelihood that physical manipulation of the screen, such as bending, will lead to an increase in at least one of the screen pores and thereby reduce the bubble point. Therefore, the hypothesis for this study was that the more deformation a screen undergoes, the more likely it is that the bubble point is degraded; making the bend radius inversely proportional to bubble point reduction.

## **III. Test Description**

### **A. Experiment Architecture**

In determining the capillary capability of a surface tension screen, a pressure differential is created across a fully wetted screen until the liquid barrier is penetrated by pressurized gas. While simple in concept, the execution includes varying issues of complexity including: choosing compatible test fluids and materials which also closely approximate the behavior of liquid propellants, developing a gas-tight seal on the test cells without impacting the integrity of the screen pores, testing the same screen test segment in different cells, filling and draining the cells during testing, measuring pressure with an accuracy of hundredths of psia, testing in a microgravity environment, and conforming to NASA flight test safety standards. This section of the paper will explore, in detail, the general scope and design of the project.

The test setup was designed under strict requirements, since the testing requires a microgravity environment; available to the team through the NASA Systems Engineering Educational Discovery program. For this program, NASA allows two flight days on the "Zero-G" commercial microgravity test lab. Each test flight consisted of roughly 30, 20 second microgravity test cycles, or flight parabolas, with three test operators allowed to assist. Nominally, the test flights were broken into two 15 parabola spans with a 1-g reset phase in-between (Figure 3) allowing for a best case total of 60 microgravity cycles. However, several of the 60 test cycles were used in allowing test conductor acclimation to microgravity and were also used for test setup calibration. In addition, the number of test parabolas was dependent on flight conditions for the day and the microgravity quality varied from parabola to parabola. Due to these considerations, the assumption was that 20 adequate-quality data points could be collected per flight day.

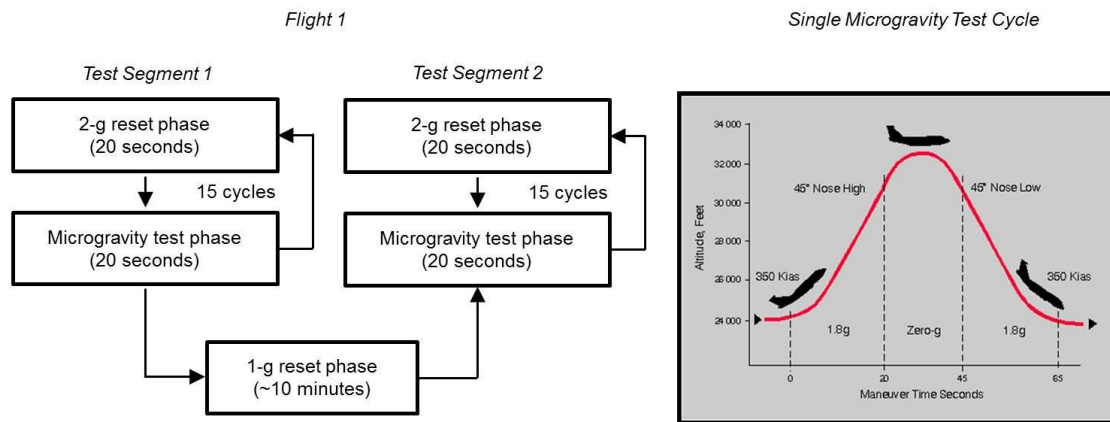


**Figure 3. Single microgravity flight test description (left) and a single microgravity test cycle (right).<sup>6</sup>**

Three different surface tension screens were evaluated in this study: 22x110 titanium, 30x160 titanium, and 325x2300 stainless steel (Figure 4). The screens were chosen to represent two common alloy types for both lower and higher acceleration mission types. For high acceleration missions, finer screens with higher capillary capability are required. Missions where material compatibility with the propellant, primarily oxidizer, is a concern, a more coarse titanium screen is generally used. In general, the type of PMD and surface tension screen used is a complex choice which depends on many different mission and spacecraft parameters.

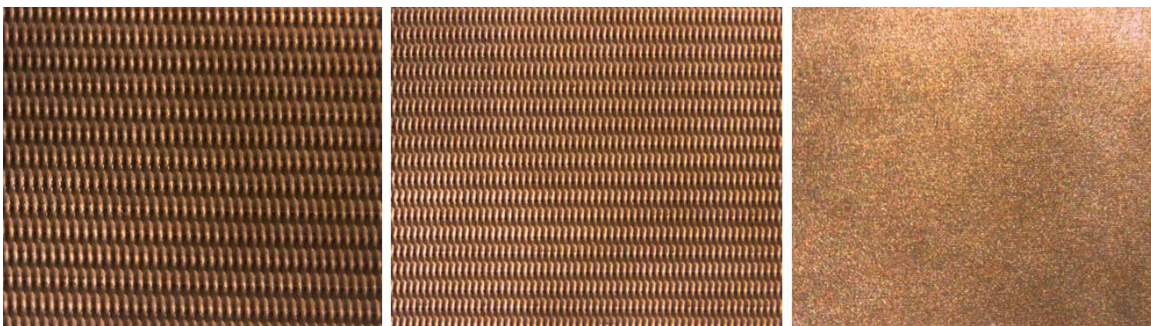


**Figure 4. Close-up views of the three surface tension screen types evaluated in this study: 22x110 Titanium (left), 30x160 Titanium (center), and 325x2300 stainless steel (right).**

The number of test runs was limited by the scope of the microgravity program; therefore, four test samples for each of the three screen types were tested simultaneously to increase the data sample size. Each of the two flights had two distinct test segments (prior to and after the 1-g turn reset phase) allowing for the test samples to be reset a total of four times – naturally leading to the possibility of testing 4 different radii of curvature. The result was a total of 12 test cells (Figure 5 - left). The four radii of curvature explored in this research were: 4", 3", 2", and 1".

The experiment design permitted screens to be swapped out by first creating a chamber with very thick walls, so that precision accuracy was not required for placing the screen; and second, by holding the cells closed with latches to create a good seal quickly. The quick-seal boxes all had adjustable latches that allowed a screen to be quickly removed and its replacement attached in in less than 30 seconds. This quick-release mechanism was critical for successfully swapping the 12 screens into different curvatures within the 12 test cells during the 10 minute 1-g test reset time.

To run 12 bubble point tests simultaneously during a short 15-20 second period, a complex plumbing system was designed (Figure 5 - right). The external interfaces and internal mechanics of each cell, both the curved and flat test cells, will be described in subsequent sections.

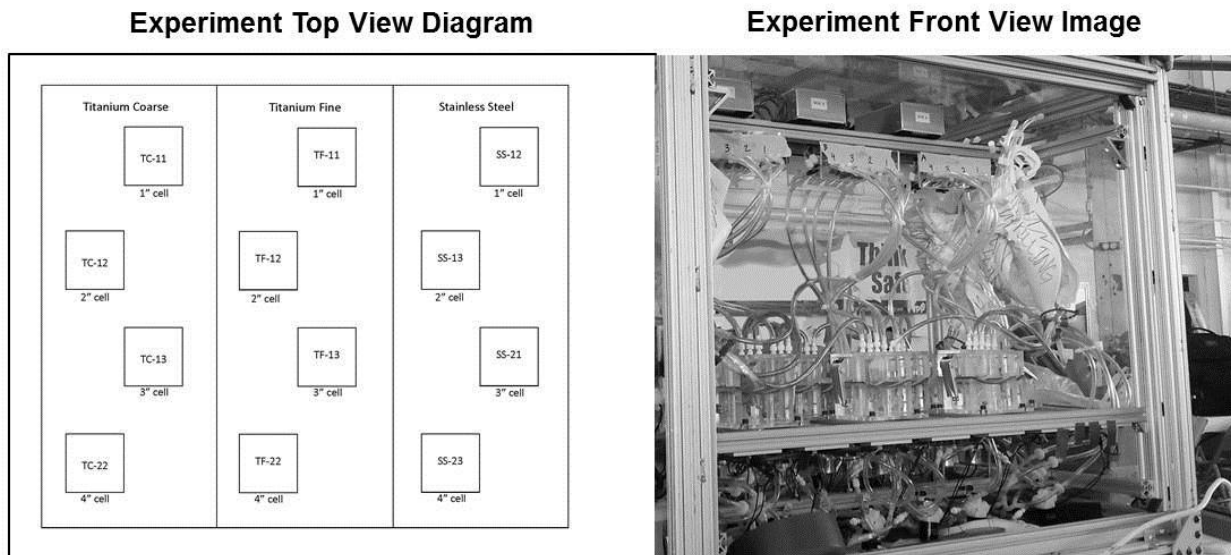


**Figure 5. Zero-g flight experiment pre-flight layout. Top diagram of twelve test cells (left) and photo of experiment plumbing and cell orientation (right).**

Data were collected using silicone-diaphragm Wheatstone bridge pressure-differential transducers. Their signals were amplified using instrumentation amplifiers attached to printed circuit boards. To reduce error and protect against a broken transducer, two transducers recorded the pressure differential in each chamber. Due to variation across individual transducers, the pressure measurement system was calibrated before and after flight using hydrostatic columns of known height. Data from the transducers were collected using two Arduino megas, while data collection, pumps, and solenoids were controlled through hand-operated switches, due to their simplicity, reliability and flexibility.

Finally, a decision matrix was used in determining the working fluid for the experiment. The team evaluated using Ethanol, Isopropyl Alcohol (IPA), and Performance Fluid. Each of the fluids were scored and compared in the categories of: availability and cost, material compatibility, safety, and industry experience with the fluid properties (contact angle consistency and surface tension) representing the largest weight. The comparison led the authors to use IPA as the working test fluid in this study.

## **B. Flat Screen Testing (Nominal Testing)**

The industry baseline for surface tension screen bubble point testing is to complete the capability tests in 1-g with the screen in a flat orientation regardless of the orientation in which the screen is used (curved, warped, or flat). Values obtained from the flat orientation screen testing are reported as the nominal performance capacity; though a knockdown factor is typically applied, mainly to compensate for manufacturing variations. In this study, the screens were also tested in a flat orientation in a 1-g environment, using the same methodology as industry, to establish the nominal capillary capability of each of the three screen types.

For the flat screen testing, a leak-tight acrylic cell was produced which contains a screen divider in the center of the cell as the unit under test. The bottom segment of the cell is slowly filled with IPA until the screen is completely wetted by the liquid and the bottom of the cell is 100% full (Figure 6a). Air is then pumped into the lower half of the cell displacing a small amount of liquid forming a layer of gas along the bottom surface of the screen under test. Since the IPA can cross a wetted screen with no resistance and the gas cannot, the liquid forms a shallow puddle above the screen equivalent to the volume of the gas bubble below the screen. The liquid puddle above the screen ensures that the screen remains wet during testing while the gas bubble under the screen eventually covers the entire

screen area. The configuration before the bubble point test begins is shown in Figure 6b.

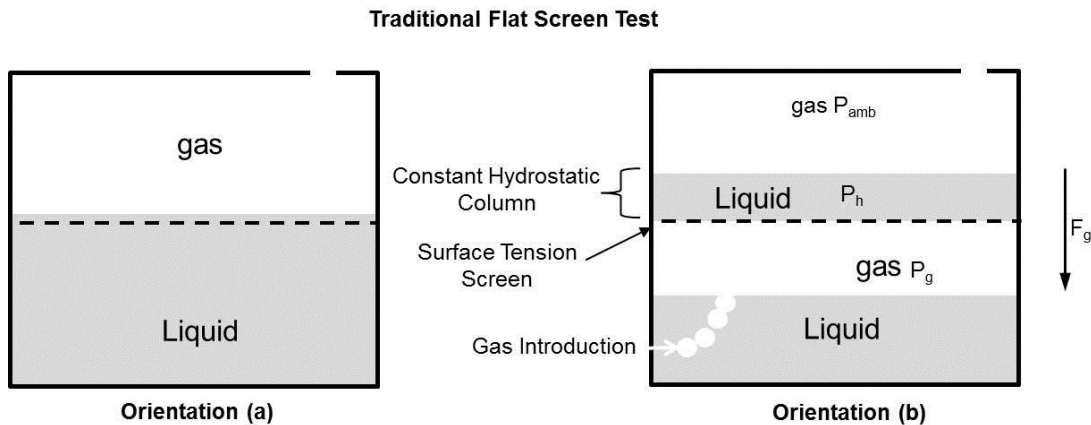


**Figure 6. (a) Flat test cell initial orientation. (b) Flat test cell orientation just prior to the bubble point test. The liquid above the screen maintains screen wetness and the gas bubble under the screen ensures that the entire screen is included in the test.**

In orientation (6b), a hydrostatic column is developed by the liquid above the screen. However, because the screen is perfectly flat, the hydrostatic pressure is constant at every point on the unit under test ensuring that the conditions for the screen are uniform. As the bubble point test begins, additional air is pumped into the lower half of the test cell increasing the gas pressure. Eventually, once the bubble point is reached, any additional pressure introduced into the bottom of the cell will force gas across the screen boundary and prohibit any more pressure from building. The pressure differential between the top of the cell and the gas in the bottom of the cell at this equilibrium condition is screen’s nominal bubble point and is given by the equation:

$$\Delta P = |P_g - (P_h)| \quad (2)$$

The test cell consists of two precisely machined half-cell acrylic segments which can be clamped together with the screen in-between (Figure 7). The screen is adhered to a silicon lining which, when compressed between the two cell walls, creates a leak-tight boundary along the edges. The cell contains access ports which allow for IPA or air to be pumped into the cell appropriately. Other test cell ports are connected to high accuracy pressure transducers to measure the results of the test and allow for venting of the top of the cell where pressure shouldn’t accumulate. The testing was done repeatedly, in series, to collect a statistically significant sample size of bubble point results. Time between tests was taken to allow the liquid on the screen to settle, eliminating the possibility of collecting bubble point results measuring the reseal bubble point rather than the actual nominal screen capability.



**Figure 7. Picture of the actual flat-screen nominal testing cell. The latches**

The flat screen normalization tests were done in isolated test units prior to flight. Each of the three different screens were tested 10 times to gather a significant number of data points; primarily to demonstrate repeatability. In all, four screens for each of the three screen types (12 total) were tested. The end result is an average nominal value for each screen and demonstrates the baseline capillary capability (or bubble point) for each of the 12 screens.

### C. Curved Screen (Zero-Gravity Testing)

As mentioned in previous sections, the alteration of the screen orientation via bending or warping can lead to the manipulation of the screen's triangular capillaries thereby affecting the bubble point of the screen. The goal of the experiment is to complete bubble point tests for screens of varying degrees of curvature and compare the results to the nominally flat tested screens.

The procedure for testing the screens in a curved orientation is virtually identical to testing the screens in a flat orientation. The screen must be fully wetted, one side of the screen must be in full contact with gas, and the same side must have the pressure incrementally increased until the gas bubbles through the screen. However, when the screen is in a curved orientation, the effect of gravity on the test setup is no longer uniform. There are two important differences with respect to gravity when the screen is being tested in a curved orientation. If a puddle of liquid exists above the screen for the purpose of maintaining a completely wetted state, the hydrostatic pressure will vary as a function of the height of the liquid (Figure 8b). Applying the nomenclature in Figure 8, the bubble point in 1-g is:

$$\Delta P = |P_g - P_h(H)| \quad (3)$$

Because the hydrostatic head resists the flow of gas through the screen, as does the bubble point, the gas will ultimately bubble through the screen at the point where the hydrostatic pressure is lowest. In this case, not all pores on the screen are tested equally. If the puddle is removed and the screen is prewetted, gravity will reduce the wetting of the screen corners as the fluid is pulled down into the center; also misrepresenting the capacity across the entire screen. For these two reasons, the curve screen tests require a microgravity environment.

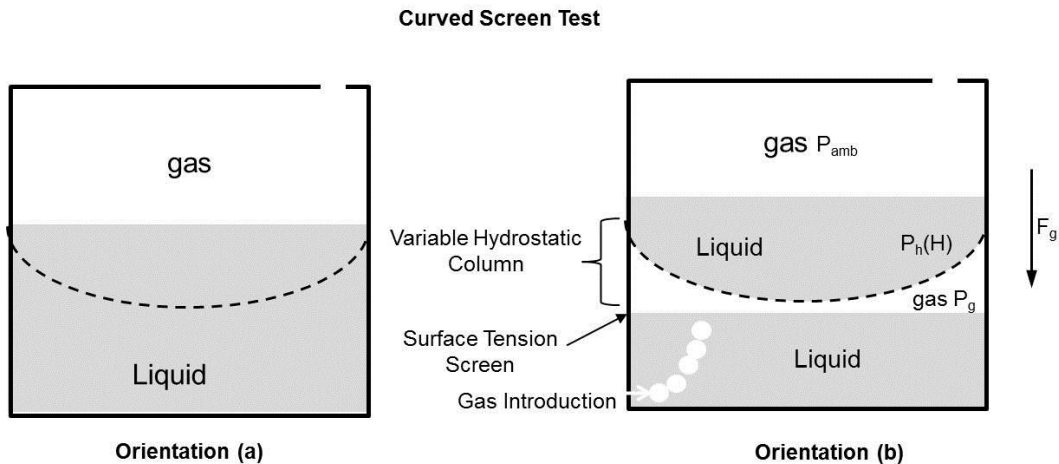


**Figure 8. (a) Curved test cell initial orientation. (b) Curved test cell orientation just prior to the bubble point test. The liquid puddle above the screen maintains screen wetness and the gas bubble under the screen ensures that the entire screen is included in the test.**

Each of the curved cells consists of two precisely machine acrylic halves and 5 total testing ports (Figure 9). The radius of curvature is imposed on the screen by the matching convex (top half) and concave (bottom half) machined curvatures of the cell interface. The halves are mechanically latched to fix the screen into place for a leak-tight fit.

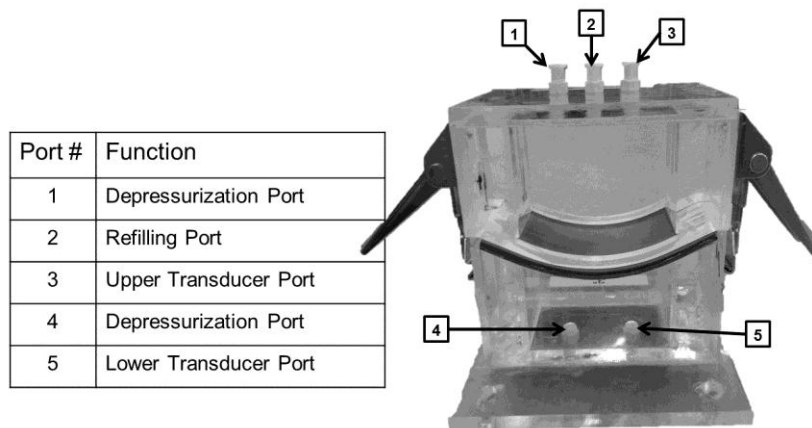


**Figure 9. Example of a test cell for curved surface tension screens with the five test ports described.**

Prior to the microgravity flight, the cells were prepared with each of the 12 screen test samples (four samples of three screen types) placed in the test cells for the first half of the flight. Each of the screens were submersively wetted, after which a small IPA puddle was developed above the screen to maintain complete wetness during flight. Each of the cells were latched, sealed, and underwent inspections to ensure proper function.

During the microgravity flight, the 12 screen samples were tested for bubble point simultaneously at fixed curvatures. Aquarium pumps (one per cell) were used to pressurize the bottom half of the test cell during the zero-g segment until the bubble point was reached, while pressure transducers recorded and stored the pressure data during the test. After each zero-g test segment, both the top and bottom of each cell was depressurized and reset for the next test run, or zero-g parabola. This process was repeated for the first ~12 parabolas until the 1-g turn-around phase of the flight. During the 1-g turn-around phase of the flight, the rig was opened and all the surface tension screens were swapped into a different test cells with different radii of curvature; allowing each screen to be tested at two different radii of curvature in a single flight.

Over the two zero-g flights, each with 2 test segments separated by the 1-g turn-around, the screens were each tested at 4 different radii of curvature. The final test results include three screen types with four screen samples of the same screen type each tested for four radii of curvature. Due to variation in the flight plan and the occasional technical issue (i.e. temporary pump failure, cell leakage, etc.), each sample did not receive the same bubble test quantity. However, in most of the tests, enough data was collected to minimize uncertainty in the results.

## IV. Results

### A. Flat Screen Testing (Nominal Results)

As outlined in section III B, each of the screen samples were tested in a flat orientation to ascertain the nominal performance of the screen section. Flat screen testing is the standard industry process for determining a screen's capillary capability, mainly because testing screens in the final integrated flight orientation isn't possible in 1-g. The rest results were remarkably consistent when time was allowed between bubbling to reduce the potential for measuring the effects of reseal bubble point. Figure 10 illustrates an example of a pressure trace as the bubble point is measured.

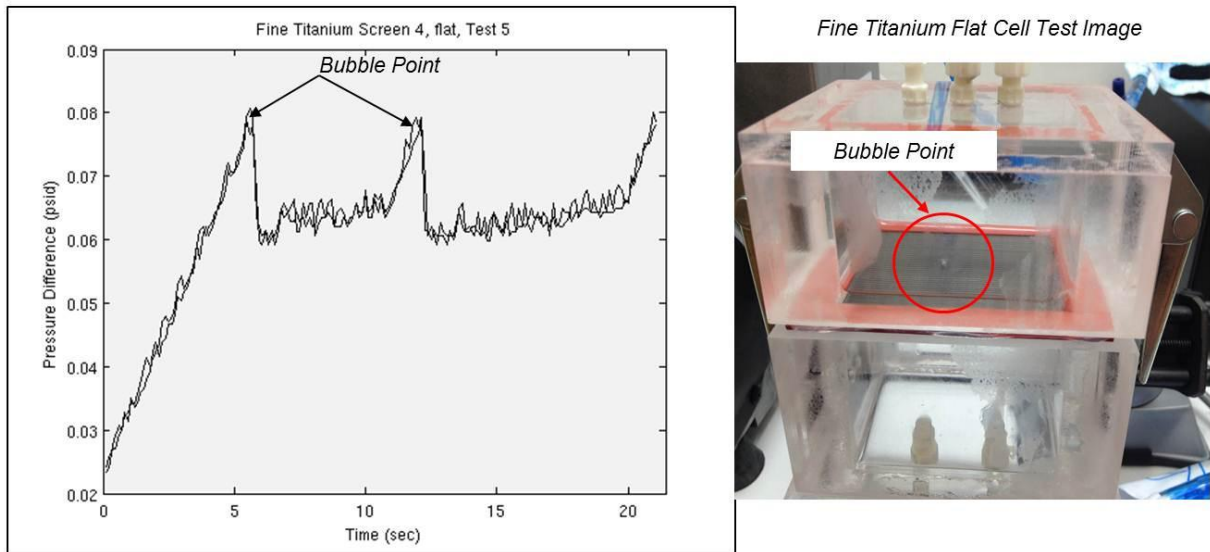


**Figure 10.** Example pressure trace during a flat screen bubble point test for a 30x160 Titanium screen (left) with a corresponding image capturing the bubble point in action (right).

The tests were repeated 10 times for each of the 12 screen samples, at a temperature of 75 °F, to develop a statistically repeatable result. The resulting nominal screen performance data were then used as a benchmark of comparison for the eventual curved screen testing. Table 1 summarizes the results for each of the three screen types in units of psid.

| Screen Type | Flat Orientation Bubble Point |
|-------------|-------------------------------|
| 22x110 Ti   | 0.070 psid                    |
| 30x160 Ti   | 0.086 psid                    |
| 325x2300 SS | 1.024 psid                    |

**Table 1.** Compiled results of the baseline flat orientation surface tension screen bubble point testing. The numbers are the average result for a sample size of 10 test cases.

## B. Curved Screen Results

After each of the 12 screens were tested for nominal capillary capability in 1-g, the screens were prepared for testing in a curved orientation. The curved screen testing was performed in microgravity and the test sequence was highly automated due to the interaction limitations in the test environment. Each test cycle was initialized by computer program and then ran autonomously until the start of the next sequence. During the 1-g test reset period, the cells were opened and the screens were very carefully swapped into a different cell with a different radius of curvature for the next test segment. In all, each screen had the potential for roughly 10 test cycles at a given curvature; of which there were four. It should be noted that the screens were not tested in progressively curved orders. In other words, a screen could see a 1 inch curvature test sequence prior to a 3 inch curvature test, and so on.

Several video cameras were set up to record selected cells during the flights – usually the 1 inch curvature cells where the most dramatic results were anticipated. The video proved to be critical in determining the data markers of healthy test runs as well as those that were unusable. It was suspected that the test pressure curves

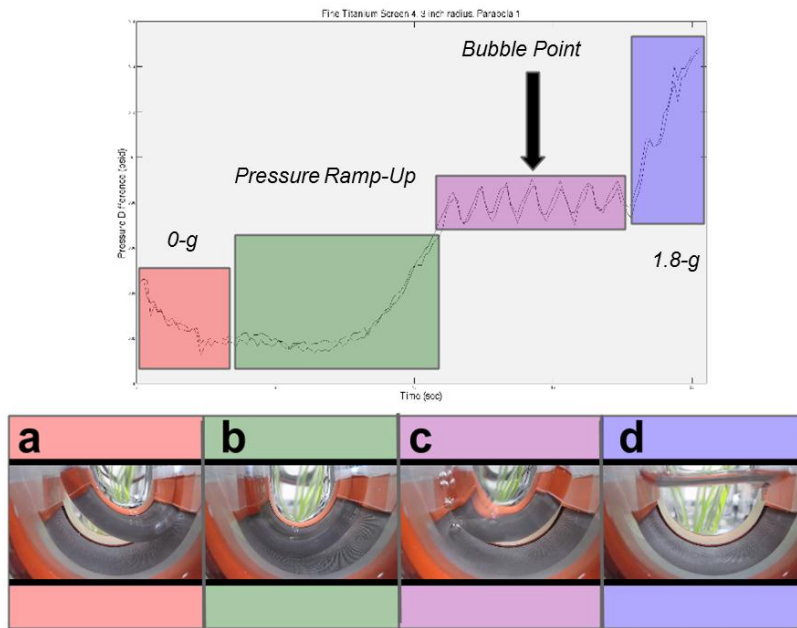


**Figure 11. Example of a bubble point test cycle in microgravity showing: (a) the zero-g transition phase, (b) the pressure ramp-up phase, (c) the bubble point saw-tooth, and (d) the 1.8-g test cycle phase.**

Initially, the data from each of the four screen samples for a specific screen type was analyzed and averaged to form plots of bubble point vs radius of curvature; Figure 12 is an example of the data set for the 325x2300 stainless steel screen samples. As demonstrated by the data, the stainless steel screen consistently demonstrated the trend of bubble point capability reduction as a function of decreasing radii of curvature across the four samples tested. The range of capability reduction at the most stressing curvature, 1 inch, is between 8% (sample 1) and 38% (sample 3).

The 30x160 Titanium screen, however, demonstrated less consistent results; though, while still showing slight trends toward performance degradation (Figure 13). Due to the higher rate in data corruption from the 30x160 screen samples, the error bars are considerably more prominent making it difficult to ascertain a specific trend. The range of capability change in the 1 inch curvature for the fine titanium is +10% (sample 4) to -21% (sample 2).

would have similar characteristics to the flat screen pressure curves. More specifically, the phases of the data would include a pressure ramp-up phase as gas is injected into the lower half of the cell as well as a “saw-tooth” pattern which would be indicative of the pressure drop as a bubble crossed the wetted screen boundary. In addition to these two characteristics, the authors predicted that the pressure would initially drop as the plane entered microgravity, as the hydrostatic column went to zero, and that there would be a pressure increase at the tail end of the data as the hydrostatic column redeveloped during the 1.80g portion of the test cycle. Figure 11 confirms the data collection phases hypothesized by the authors via the pressure curve and corresponding video data.

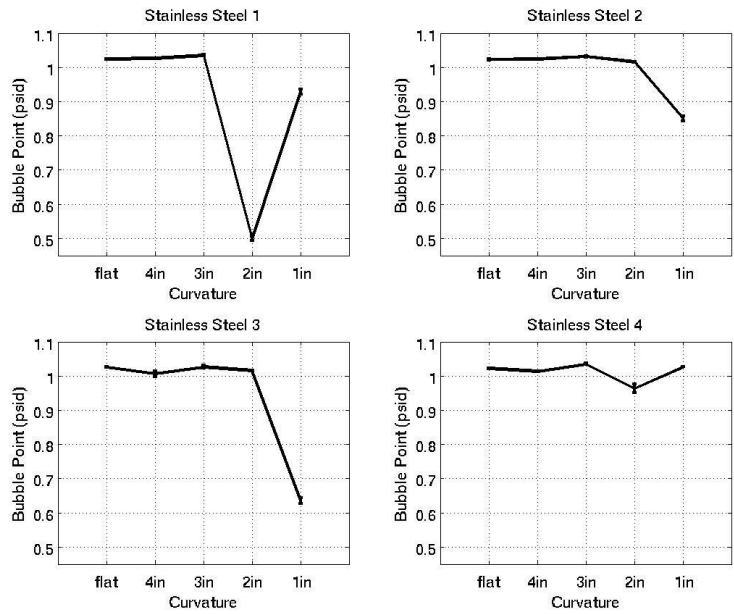


**Figure 12. Stainless steel (325x2300) capillary capability plots over varying curvature for the four different test samples evaluated.**

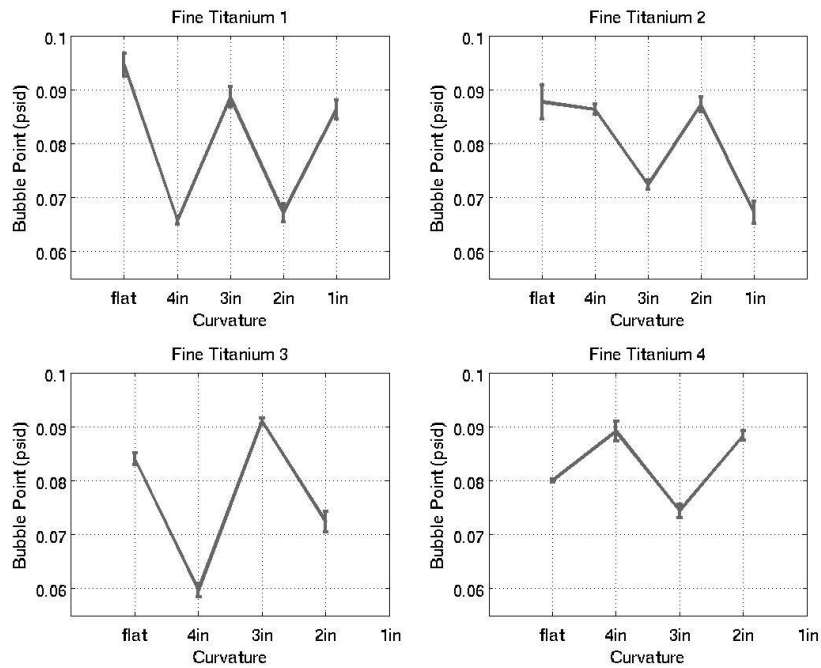


**Figure 13. Titanium (30x160) capillary capability plots over varying curvature for the four different test samples evaluated.**

Finally, the coarse Titanium weave (22x110) was very challenging from a data acquisition perspective primarily because of the low bubble point and sensitivity to all of the considerations further discussed in section IV C. As demonstrated by Figure 14, several of the screen samples have indetermined data for multiple curvature tests because of data corruption. In this case, the results are mainly a rise in bubble point as the screen curvature intensity increases – with sample 2 indicating a roughly 17% increase.

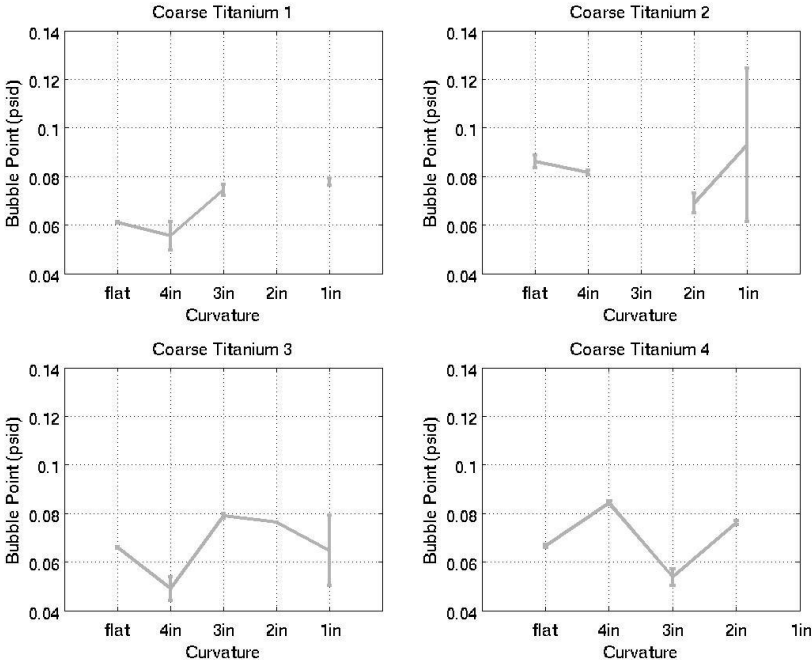


**Figure 14. Titanium (30x160) capillary capability plots over varying curvature for the four different test samples evaluated.**

Further data analysis involved combining the four samples into a single bubble point vs curvature radius line for each screen type and normalizing by the sample’s respective flat point tests. The result is the normalized change in capillary capability of the screens as a function of radius of curvature (Figure 15). The final representation of the data from this study clearly shows variation in the bubble point as the screen is warped; however, a trend of capability degradation is only moderately apparent for the 30x160 Titanium and 325x2300 stain steel screens at the more extreme curvature values. The coarse Titanium data (22x110) reveals an increase in the normalized bubble point as the curvature approaches 1 inch, albeit with significant error driven by low sample size and high variability.

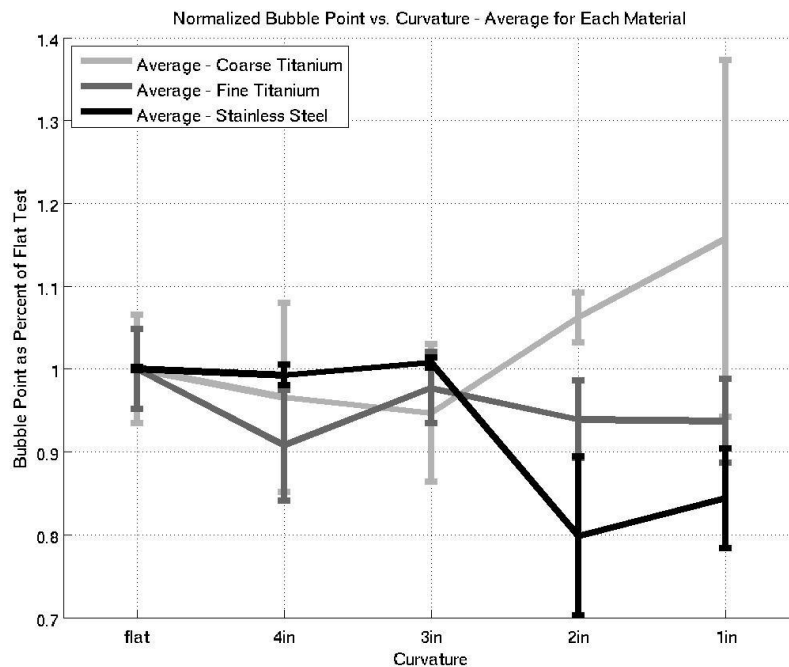


**Figure 15. Plot of each screen types bubble point normalized by the flat screen results as a function of the radius of curvature. The plot represents the combination all 4 samples for each screen type.**

### C. Results Evaluation

The results, as outlined in section IV B, Figures 12 through 15, do show a moderate downward trend as the radius of curvature decreases – i.e. as the screen is more sharply bent. However, the quantitative performance impact as a function of screen curvature is much more difficult to see. In particular, the coarse Titanium (22x110) actual demonstrates a performance improvement as the screen is curved to the 2 inch and 1 inch marks. This result may be misleading since many of the test results were removed as non-viable data due to corruption. The small sample size for the coarse titanium, and indeed some of the other screen types, led to significant error bars which may be masking the true statistical impact of screen curvature on performance. Several hundred pressure curves were measured during the test segments across the three screen types and the four screen samples; however, many of them did not yield usable data. The primary sources of corruption in the data acquisition were:

- Underpressurization of the cells via pump stalling or test cell leakage.
- Pressure transducer failure or changes in calibration with unknown root cause
- Liquid, IPA, plugs in the pressure transducer lines which introduced a bias in the readings
- Lack of data quality verification in marginal cases

One of the surprising findings from the study was the variety of pressure trends in the tests which could be considered usable bubble point results. The initial assumption was that data born of good test quality would have consistent markers which would later be used to identify which data could be used in the analysis. However, the authors found, through the correlated video data, that usable pressure curves from good tests varied in signature greatly, making the data analysis extremely difficult. Several good quality pressure curves were likely not included in the averages simply to be conservative in the reporting process.

Never the less, the data does show conclusively that the screen’s capillary capability is impacted by warping the

screen to very small radii of curvature. The change to the screen's performance is in the range of +15% to -25% of the nominal baseline. Although it's important to note that in actuality, a 1 inch curvature is well beyond what is typically seen in industry. Even a small spherical tank containing a gallery arm PMD device will usually have a radius of curvature greater than 10 inches. For all practical purposes, the data seems to indicate, based on the 3 and 4 inch curvature data, that performance variations in a typical spacecraft application will not be substantial ( $\pm 10\%$ ).

## V. Conclusion

### A. Summary

The authors of this study attempted to develop a definitive, quantitative result – or mathematical trend – for predicting the bubble point performance variation of a surface tension screen in a curved orientation. The authors found that the low sensitivity of the screen performance to screen curvature coupled with the challenging microgravity testing environment made that goal very challenging. However, the tests were successful in demonstrating that performance variations do exist under sharp curvatures. In fact, the results show that for the sharpest curvature tested (1 inch), the performance can degrade up to 25%, as shown by the 325x2300 stainless steel screen data. An additional success in this study was the compilation of solutions for common challenges for this variety of research, as outlined in section V B.

### B. Project Challenges, Solutions, and Lessons Learned

This research project has been attempted on multiple occasions by other research groups, always encountering critical challenges that had negative impact on results. The Yale/Lockheed team was able to apply the lessons learned from previous projects, predict issues, and resolve technical challenges as they were encountered. This section attempts to encompass the mitigations for technical issues common to this type of project.

- **Cell Crazeing**

Many cells quickly developed a network of cracks along their edges, seemingly as a result of repeated exposure to IPA. Though this effect did not break any cells, it seemed to weaken them and perhaps make them more vulnerable to fracture. Eventually it was determined that the laser cutting process was affecting all acrylic edges. The original solution was to coat the edges of the cells in epoxy to protect them from IPA. Eventually this became unnecessary, when changes in the cell design forced the cells to be machined instead of laser cut.

- **Screen Sealing**

The edges of the screens were glued to rubber seals in order to prevent cells from leaking. However, any glue on the screen lowered the bubble point for that particular region, and in early tests of the cells, bubbles usually emerged first in areas where glue was on the screen. To avoid this problem, glue was applied only to sections of the screen that would be completely covered by rubber. As a result, the thickness of the cells – and thus the width of the rubber edges – was increased to  $\frac{3}{4}$  in. This thickness was too large for the laser cutter, so cells had to be machined.

- **Developing Cell Pressure**

Initially, hand pumps were used for the test article, but they made it difficult to apply pressure smoothly and to determine the pressure at the bubble point, even under lab conditions. These pumps were replaced with electronic pumps that could deliver a smoother increase in pressure.

- **Temperature Recording**

The original plan for measuring temperature was to use a resistive thermal device in several of the cells. The RTD could be connected to a voltage divider, allowing an Arduino microcontroller to measure the change in resistance, and thus temperature. No significant changes in temperature were expected, so changes in the resistance would be very small. The Arduino's analog input could measure between 0 and 5 volts, and at this range, changes in voltage produced by the RTD and voltage divider circuit would be smaller than the Arduino could detect. The RTD

was simply replaced with a small thermometer located on the apparatus structure, allowing the temperature to be manually recorded at various points in the experiment.

- **Screen Quality**

Even minor damage or bending would lower the bubble point. Several procedures were developed to trim, glue, seal, transport, and otherwise handle the screens to keep the bubble points as high and as uniform as possible. The project's data, which recorded bubble points consistently above the industry standard, demonstrate that these procedures were successful.

- **Screen Swapping**

The ability to change the screen curvatures in flight provided a much richer understanding of the phenomenon under study but presented a number of technical challenges. It required a system of latched cells that could be manipulated by experimenters through several double-layered sets of gloves. Additionally, a draining and refilling system was put together to minimize IPA leakage into the main box while ensuring that screens would stay wet after the swap.

- **Screen Dry Out and Cell Draining**

Fluid in the bottom of the cells can create difficulties in generating pressure; a partial loss of fluid in the top would make it more difficult to discern visually that pressurization was occurring successfully and a total loss would have risked screen dry-out, invalidating the test. The in-flight practice of sealing the top half of the cell before draining the bottom minimized movement of fluid to the bottom of the cell.

### **Acknowledgments**

This research was completed as part of the NASA Systems Engineering Educational Discovery (SEED) program; a joint effort involving the NASA Johnson Space Center, Yale University, and Lockheed Martin Space Systems Company. Christine Stewart, Jonathan Braun, and Dr. Steven Irons served as the principal investigator, subject matter expert, and Yale faculty advisor, respectively. The student flight team consisted of Emma Alexander, Michael Cruciger, Phillip MacEachron, Nafeesa Khan, and Sara Flintgruber. Ground operations were supported by Manjari Randeria. Student researchers included Noah Conally, Brianna Chrisman, Katherine Lawrence, Zachary Brunt, and Joseph O'Rourke. Funding for this work was provided by the NASA SEED program, the Connecticut Space Grant Consortium, and the Yale physics and engineering departments. Test materials and technical review was provided by Lockheed Martin Space Systems Company.

### **References**

<sup>1</sup>Jaekle, D. E., Jr., "Propellant Management Device Conceptual Design and Analysis: Vanes", AIAA-91-2172, 1991.

<sup>2</sup>Jaekle, D. E., Jr., "Propellant Management Device Conceptual Design and Analysis: Sponges", AIAA-93-1970, 1993.

<sup>3</sup>Jaekle, D. E., Jr., "Propellant Management Device Conceptual Design and Analysis: Traps and Troughs", AIAA-95-2531, 1995.

<sup>4</sup>Jaekle, D. E., Jr., "Propellant Management Device Conceptual Design and Analysis: Galleries", AIAA-97-2811, 1997.

<sup>5</sup>Jurns, J. M., et. al., "Bubble Point Measurements With Liquid Methane of a Screen Channel Capillary Liquid Acquisition Device", NASA/TM—2009-215494, 2009.

<sup>6</sup>Images courtesy NASA.